A Numerical and Experimental Investigation of a Gurney Flap on a Newman Airfoil

SBLT Timothy M. Laughlan, RAN*

University of New South Wales at the Australian Defence Force Academy, Canberra, ACT, 2600, Australia

A Gurney flap is a form of high-lift device, used to increase the lift-to-drag (L/D) ratio of a wing. The interesting thing about the Newman airfoil shape is that it encounters a continuous adverse pressure gradient aft of the maximum thickness-to-chord (t/c) position. This causes the airfoil to be prone to separation near the trailing edge. The provision of a Gurney flap alleviates this, since it gives the airfoil an effective camber. The aim of this research was to examine the effect of the height of a Gurney flap in alleviating this separation and thus to improve the L/D ratio. This was achieved through wind tunnel experiments, including surface-oil-flow-visualisation to see where the flow separates on the airfoil. Computational Fluid Dynamics (CFD) simulations were also conducted to compare the experimental data thus validating the CFD and also validating previous research including the hypothesised trailing edge flow structure around a Gurney flap.

Contents

*4th Year Aeronautical Engineering Student, ZEIT4501. Compiled using LaTeX 2_ε version 2.9

Nomenclature

L	Lift Force, [N]
D	Drag Force, [N]
t	Thickness of Airfoil/Wing, [m]
h	Gurney flap Height, [% chord]
c	Chord Length, [m]
α	Angle of Attack, [°]
Re_c	Reynolds number (based on the airfoil chord length)
C_l	Lift Coefficient (per unit span)
C_d	Drag Coefficient (per unit span)
$\Delta\Gamma_G$	Increase in Circulation due to Gurney Flap, [m^2]
Δ_∞	Circulation of Airfoil (no flap), [m^2]
k	Base Pressure Parameter
$\Delta\bar{\omega}$	Constant defined by Gai[1]

I. Introduction

The aerodynamic efficiency of an airfoil is measured through it's L/D ratio. The desire to improve performance by increasing wing loading and thus the maximum lift coefficient of wings without changing other flight parameters led to a need for high-lift devices[3]. In the past, a significant amount of research has been invested into the design of high-lift devices for use on aircraft to maximize lift. An effective high-lift system allows for a higher stall speed and increased takeoff and landing performance. If high-lift devices are permanently deployed, the aircraft becomes capable of transporting a greater payload for a given gross weight. This allows the aircraft to reach cruise altitude faster, resulting in a more fuel-efficient flight[4,5].

A cheap, simple, permanently deployed high-lift device such as the Gurney flap[6], increases the lift on the airfoil since it gives the airfoil an effective camber. There is a small increase in drag however, the lift increase is much greater than the drag increase up to an optimum Gurney flap height, thus giving the airfoil an overall improvement in the L/D ratio[1]. If one can obtain double the lift by fitting a 0.01c Gurney flap to the trailing edge of an Unmanned Aerial Vehicle (UAV), mission requirements could be extended significantly.

II. Experimental Investigation

II.A. Models, Equipment and Techniques

Wind tunnel experiments were conducted on a Newman airfoil-shaped[2] wing with Gurney flap attached [Fig. 1(a)]. The wing had a maximum t/c ratio of 0.1. The two Gurney flap heights (h) examined were $0.024c$ and $0.04c$. The heights of the Gurney flaps needed to be less than the thickness of the boundary layer at the trailing edge. If they extend beyond the boundary layer, the large drag increase causes an unsteady wake to form[1]. Trip strips were used to ensure a turbulent boundary layer over the whole model to induce a turbulent boundary layer over the wing to simulate the flow over a full-scale aircraft since the Reynolds numbers were comparatively low (in the transition range for the airfoil). These heights were calculated based on the turbulent boundary layer equation[7]:

$$\delta = \frac{0.37c}{\sqrt[5]{Re_c}} \tag{1}$$

Fig. 1(b) shows the CATIA design of the model[8]. The experiments were repeated 3 times and 10 Force Balance readings were averaged for each angle of attack (α). The Force Balance was calibrated[9,10,11] and the procedure and results can be found in the Project Specific Deliverable (PSD). The Reynolds numbers examined were $Re_c = 1.54\times10^5$ (20 m/s) and $Re_c = 2.31\times10^5$ (30 m/s) taking the 1976 Standard Atmosphere conditions of Canberra's altitude. Once the experiments were conducted, the data was analysed and the lift coefficient (C_l), drag coefficient (C_d) and L/D ratio were computed and plotted. The experimental results are plotted under 'Comparison of Results'. The full details of the Experimental Investigation can be found in the PSD.

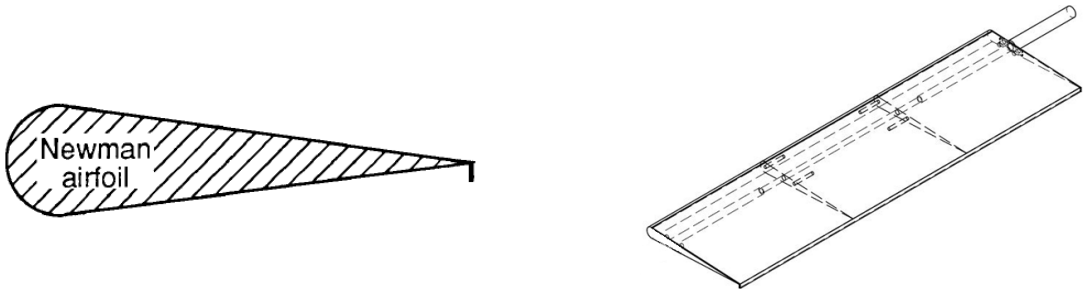

(a) Newman airfoil with Gurney flap[6]. (b) CATIA wind tunnel model design[8].

Figure 1. Airfoil and model.

II.B. Experimental Error

There are always various forms of error associated with experimental work. The wind tunnel boundary corrections[12,13,14] such as blockage and streamline curvature were made to the raw data so that the wing was in a 'far-field' and could be compared to the CFD. Various other errors included calibration error, model warp and twist, imperfections in tunnel such as leaks and chips, pitot probe error, flow inconsistencies across and along the test section and human error when measuring α. For the full error analysis, refer to the PSD.

III. Numerical Investigation

III.A. Geometry, Mesh and Setup

The CFD package 'ANSYS' (including 'Fluent') was used for the CFD simulations. A 2D geometry was created in a far-field of 20 chord lengths. A 2D geometry was decided to reduce the mesh size and thus computational time. The results are comparable to the experiments since C_l and C_d are dimensionless. The grids were generated using 'ANSYS Mesher' and consisted of 330000 cells. This contained 500 points on the airfoil wall. Fig. 2 shows the geometry and mesh of the Newman airfoil with $0.04c$ Gurney flap. The geometry and mesh were slightly modified for the no flap and $0.024c$ cases.

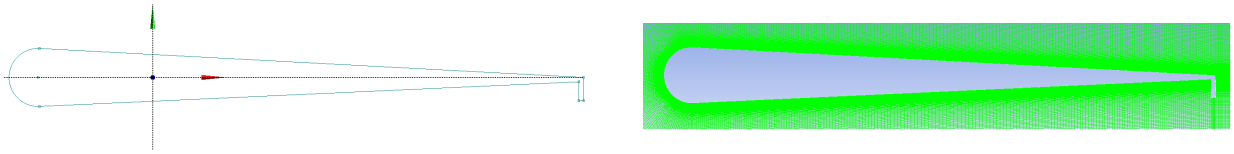

(a) Geometry. (b) Mesh.

Figure 2. Geometry and mesh used in the $0.04c$ Gurney flap simulations.

III.A.1. Grid Independence Study (GIS)

A GIS was conducted, including a Richardson Extrapolation, to estimate the 'exact' (i.e. infinite grid spacing) value of the C_d (at $\alpha = 0°$). This proves if the solution of the fine grid was within the 'asymptotic range of convergence' and thus independent. The GIS calculated an error of 4.8% in the fine grid solution. The details including the mathematics of the GIS can be found in the PSD.

III.A.2. The Wall y^+ Value

The wall y^+ value is a dimensionless wall distance for a wall-bounded flow and gives an indication of the mesh refinement as the airfoil is approached from the far-field. For far-field airfoil flows, the wall $y^+ \leq 1$. Fig. 3 shows the wall y^+ values of the grids used in the simulations.

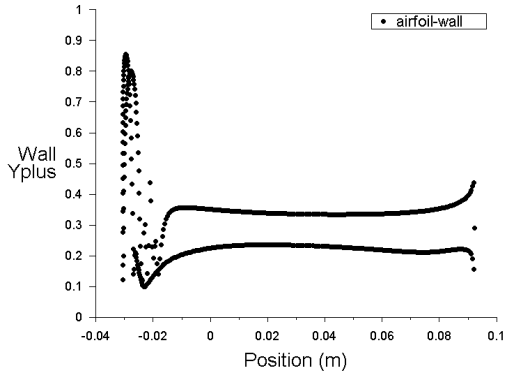

(a) Newman airfoil (no flap).

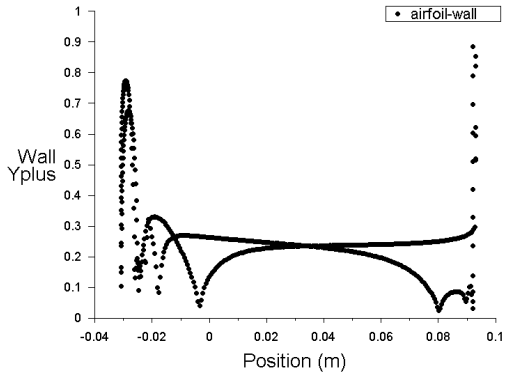

(b) 0.04c Gurney flap.

Figure 3. The wall y^+ values of the grids used in the simulations.

It can be seen in Fig. 3 that all mesh cells at the surface of the airfoil have a wall y^+ value of < 1.

A pressure-based, steady, planar solution was setup in 'Fluent'. All parameters were varied to simulate the experiment most accurately. For example, the air density, air viscosity and reference values were all matched to the experiment conditions.

III.A.3. Turbulence Model

The Shear Stress Transport (SST) $k - \omega$ (2-equation) turbulence model was selected as the best suited turbulence model for this problem and according to Versteeg & Malalasekera it 'gives superior performance for adverse pressure gradient boundary layers'[15].

III.A.4. Solution Method and Convergence

A Pressure Implicit with Splitting of Operators (PISO) algorithm was used as 'it is an extension of 'SIMPLE' with an additional...pressure correction equation to enhance convergence'[16]. Second order equations were used for 'Pressure', 'Momentum', 'Turbulent Kinetic Energy' and 'Specific Dissipation Rate' as second order solution methods are more robust than first order and are more numerically accurate[16]. Third order equations were too time consuming to solve and the level of accuracy required was achieved with the second order equations. All residual levels were set to 1×10^{-5} and are within the range of comparable literature. No under-relaxation factors were used.

The solutions were ran until the above mentioned level of convergence was achieved, writing C_l and C_d to a file. Other convergence monitors such as mass flux was also monitored to ensure a converged solution. Once the solutions converged, the C_l, C_d and L/D ratio were recorded and plotted. The CFD results are plotted under 'Comparison of Results'. The full details of the Numerical Investigation can be seen in the PSD.

III.B. Numerical Error

There are various computational errors that arise within CFD simulations and are the crux of the variation between the experimental and numerical results. The errors are summarised below[15]:

- **Discretisation errors** arise when an exact solutions to equations can not be obtained and are approximated.
- **Round-off errors** exist due to the difference in machine accuracy of a computer. All simulations were run using the *double precision* option (uses 15 significant figures) rather than just 7 for the *single precision* option.
- **Iteration or convergence errors** arise when a solution converges to the residual levels set and is believed to be 'converged' however, it is not a solution that has fully converged on a finite grid.

- **Physical-modelling errors** arise when there is no such computational model to accurately model the desired problem.
- **Human errors** arise from mistakes made by the computer operator at one or several of the crucial steps mentioned above.

Fig. 4 illustrates the impact of each error as iteration/time step count increases[15]. It can be seen in Fig. 4(b) that the total CFD error increases exponentially when the iteration count becomes large and can explain the variation in the CFD results discussed in the next section.

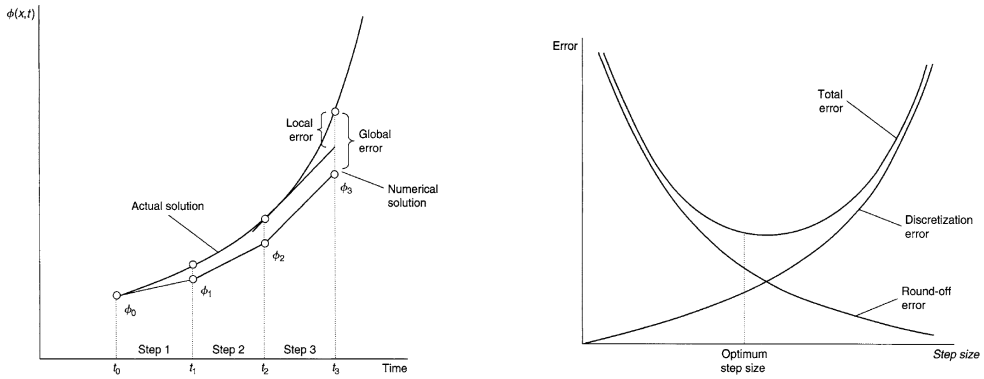

(a) Discretisation error representation.

(b) Impact of various computational errors.

Figure 4. Error vs. Iteration/Time Step[15].

For the full error analysis, refer to the PSD.

IV. Comparison of Results

A comparison between the Newman airfoil (no flap) and 0.04c Gurney flap is herein as it was the best way to draw valuable conclusions. The 0.024c results can be seen in the PSD.

IV.A. Lift Coefficient

Fig. 5 displays the experiment and CFD lift coefficient plotted against angle of attack for the no flap case and 0.04c Gurney flap case. The data points were plotted with a 5^{th}-order line-of-best-fit. It can be seen in Fig. 5 that both CFD results have higher C_l values than their experimental counterparts. This was predicted since CFD is an 'ideal' solution whereas the experiment contained a number of 'losses'. For example, the slower boundary layer flow from the tunnel walls and the induced drag at $\alpha > 0°$ since there were small (approximately 1 mm) gaps between the tunnel and the model. The total CFD error at large iteration counts impacts the final CFD values. CFD is relatively new and the turbulence model selected simulated the problem best compared with other turbulence models like the $k-\epsilon$ model as the boundary layer did not separate along the airfoil when the surface-oil-flow-visualisation showed that it did. However, physical modelling error accounts for some variation in the CFD results.

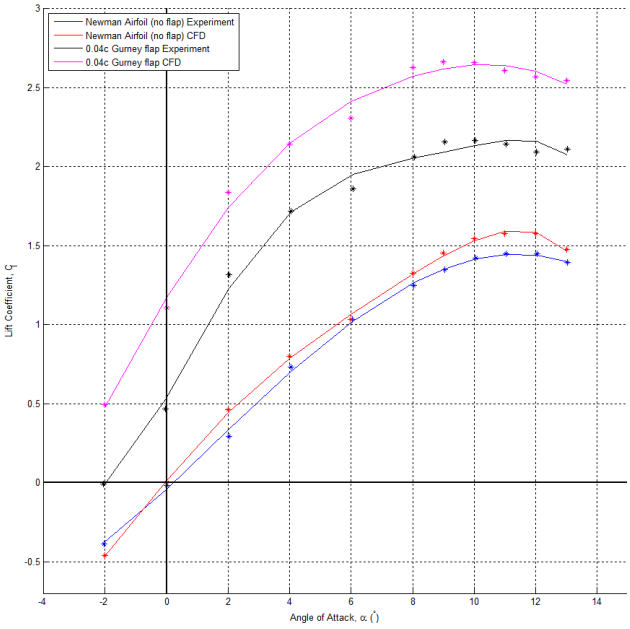

Figure 5. C_l vs. α ($Re = 1.54 \times 10^5$).

IV.A.1. Gurney Flap Effects on Alleviating Stall

Both the no flap and $0.04c$ Gurney flap lift curves are similar in shape between the experiment and CFD. An important observation is the different behaviour between the two cases at the point where stall occurs. The post stall (i.e. when $\alpha > \alpha_{stall}$) curve characteristics for the $0.04c$ Gurney flap show that the curve drops off more gradually than the no flap case. Therefore, the Gurney flap assists in alleviating stall. Table 1 summarises the lift curve characteristics of the no flap and $0.04c$ Gurney flap cases.

		$C_{l_{max}}$	α_{stall} (°)	α_0 (°)
Experiment	**Newman Airfoil (no flap)**	1.449	11-12	0
CFD	**Newman Airfoil (no flap)**	1.576	11-12	0
Experiment	**0.04c Gurney flap**	2.165	9-10	-2
CFD	**0.04c Gurney flap**	2.665	9	-3 to -4

Table 1. Lift curve characteristics (from the data points).

Table 1 illustrates that the stall angle decreases slightly from the no flap case ($11° - 12°$) to the $0.04c$ case ($9° - 10°$) and agrees with conventional stall characteristics of other trailing edge flaps. Thus, it can be concluded that the Gurney flap behaves similar to a deflected plain flap since the stall angle decreases with increasing deflection angle[7].

IV.A.2. Gurney Flap Height on Lift Production

The overall lift increase (experimental) with the addition of a $0.04c$ Gurney flap is approximately 66.9% (Table 1). This lift increase can be explained by the increase in circulation provided to the airfoil by the Gurney flap. Gai[1] conducted Gurney flap experiments and explains that the circulation ratio of an airfoil with Gurney flap to an airfoil without Gurney flap can be derived as:

$$\frac{\Delta\Gamma_G}{\Gamma_\infty} = \left[\frac{2(k-1)}{\Delta\bar{\omega}}\right]\left(\frac{h}{c}\right) \rightarrow k = \left[\frac{\Delta\Gamma_G}{\Gamma_\infty}\right]\left(\frac{\Delta\bar{\omega}c}{2h}\right) + 1 \tag{2}$$

Equation 2 explains the effectiveness of the Gurney flap is dependent on the base pressure parameter k(experimentally verified by Simmons[17] for various bluff-bodies) and the Gurney flap height-to-chord (h/c) ratio. If h/c and $\Delta\bar{\omega}$ are 0.04 and 0.01 respectively, the increase in circulation depends only on k since $\Delta\Gamma_G/\Gamma_\infty = 0.669$ (% lift increase). The expression assumes that h is small[1] to satisfy the Kutta-Joukowski Theorem[7]. This means that the addition of a Gurney flap increases the effective chord and camber of the airfoil. Additionally, if h is increased, it also increases the circulation, and thus lift on the airfoil, up to a point where the Kutta-Joukowski Theorem is violated.

If the experimental details are inputted into Equation 2, the result becomes:

$$k = 0.669\left(\frac{0.01 \times 0.125}{2 \times 0.005}\right) + 1 = 1.083625 = 1.084 \tag{3}$$

According to Roshko[18], $k \geq 1$ and is dependent on the shape of the body. Thus for Gurney flap heights in the range of $0.01 \leq h/c \leq 0.05$, the value of k may be taken as approximately 1.06 with an upper limit of approximately 1.1[1]. Therefore, a k value of 1.084 for a $0.04c$ Gurney flap is reasonable and agrees well with Roshko[18] and Gai[1].

Furthermore, the k value can be estimated from Liebeck's[6] experiment. Liebeck's data shows that for a Newman airfoil with $0.0125c$ Gurney flap, $\Delta\Gamma_G/\Gamma_\infty = 0.222$ (22% lift increase). Using these values in Equation 2 gives $k = 1.088$ which is extremely close to $k = 1.084$. If k is estimated as 1.1, for $h/c = 0.01$ the lift increases by 20% and for $h/c = 0.05$, the lift increase is 100%. In the present experiments, for $h/c = 0.04$, the lift increased by approximately 67%, which is quite comparable to the preceding estimate. Comparing this result with other researchers, Myose et al.[19] found lift increases of 25%, 36% and 47% with $0.01c$, $0.02c$ and $0.04c$ Gurney flaps respectively, which supports the theory reasonably well.

IV.B. Drag Coefficient

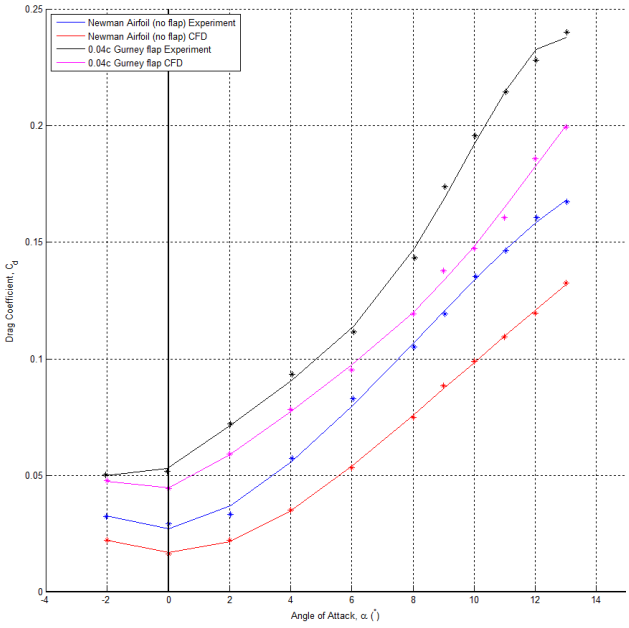

Figure 6. C_d **vs.** α **(**$Re = 1.54 \times 10^5$**).**

Fig. 6 displays the experiment and CFD drag coefficient plotted against angle of attack for the no flap case and 0.04c Gurney flap case. The data points were plotted with a 5^{th}-order line-of-best-fit. It can be seen in Fig. 6 that both CFD results have lower C_d values than their experimental counterparts. This was again predicted based on explanations provided above for the lift curves and also the 3D wing effects like induced drag on the model. As expected, the airfoil with the 0.04c Gurney flap displayed overall, a greater drag coefficient for any given angle of attack. Both configurations had very similar drag characteristics and the typical drag curve shape was observed ('bucketing' at $\alpha = 0°$ and C_d increasing with increasing α). At higher angles of attack ($\alpha > 8°$) for both experiment and CFD, the 0.04c Gurney flap curve diverged away from the no flap case, giving the Gurney flap greater drag efficiency at lower angles of attack where the 0.04c Gurney flap curves are closer to the no flap curves. Typical behaviour of considerable drag increase as Gurney flap height increased reported by Liebeck[6] were also observed.

IV.C. L/D Ratio

Fig. 7 displays the experiment and CFD lift coefficient plotted against drag coefficient (drag polars) for the no flap case and 0.04c Gurney flap case. The data points were plotted with a 5^{th}-order line-of-best-fit. Fig. 7 illustrates that both CFD drag polars have greater overall lift and drag, than their experimental counterparts as discussed previously. If the experiment and CFD are considered separately, the no flap case and 0.04c Gurney flap case converge at a point. Before this point (i.e. for low C_l and thus low α values), the curves have a dramatic lift increase. After this point, there is a dramatic drag increase and little lift production. On the contrary of lift production, another way to examine stall and thus stall alleviation is through drag increase rather than lift decrease. For example, Fig. 7 demonstrates that the maximum lift per drag increase is reached sooner for the no flap case. Therefore, the Gurney flap improved the L/D ratio considerably however, it is only effective for a small range of angles of attack, between approximately $0° < \alpha < 8°$. Beyond this α range, the Gurney flap is not as effective due to drag domination. From these findings, Gurney flaps should be restrained to race car wings due to their small effective α range where the consequences of stall are not as significant compared with aeronautical applications.

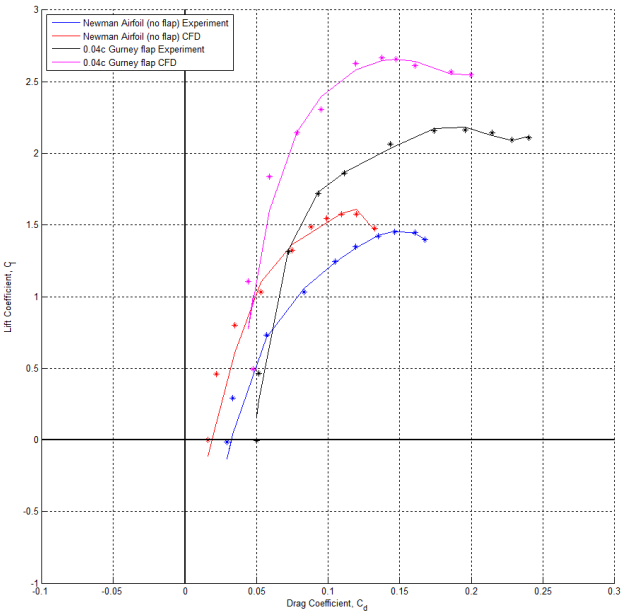

Figure 7. C_l **vs.** C_d **(**$Re = 1.54 \times 10^5$**).**

IV.D. Verification and Validation of Results

IV.D.1. Surface-Oil-Flow-Visualisation and Newman's Findings

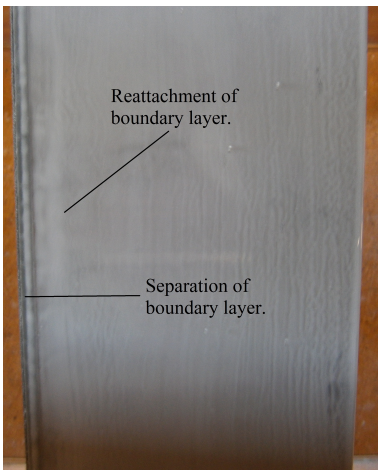

(a) 0.04c Gurney flap oil-flow ($\alpha = 0°$, $Re = 1.54 \times 10^5$).

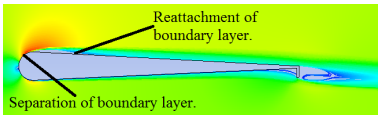

(b) 0.04c Gurney flap CFD ($\alpha = 0°$, $Re = 1.54 \times 10^5$).

Figure 8. Experiment (oil-flow) correlation with CFD.

Newman conducted experiments on the simple airfoil shape (named after him) to achieve some understanding of the behaviour of the turbulent boundary layer near separation in incompressible flow. From the experiments of the re-attachment of a turbulent boundary layer on a Newman airfoil-shaped wing, he found that at a maximum incidence of 10.5°, a tuft just behind the spoiler fluctuated in all directions at random but the tuft near the trailing edge oscillated at approximately 60° on either side of the downstream direction. This indicated that the mean velocity was no longer zero close to the surface and that the boundary layer had reattached after separation. The Gurney flap had not been invented at this time.

Fig. 8 are the results of the surface-oil-flow-visualisation (a) and CFD (b) at $Re = 1.54 \times 10^5$ and $\alpha = 0°$. This correlation between experiment (oil-flow) and CFD is a significant finding as it proves that the turbulent boundary layer does in fact separate and reattach due to the decrease in adverse pressure gradient after the maximum t/c position. The Gurney flap increases the pressure on the suction (upper) side of the airfoil, further assisting in reattachment. Fig. 8(a) also illustrates the turbulent air within the boundary layer towards the trailing edge of the wing, visible by the 'wavy' pattern of the oil. Fig. 8(a) validates Fig. 8(b) and the visible flow phenomenon occurring in the CFD is occurring in the experiment. The full-scale images of Fig. 8 can be seen in the PSD.

IV.D.2. Liebecks's Findings

Fig. 9 illustrates a comparison between Liebeck's experimental findings and the experimental findings in this research. Note that Liebeck used the symbol C_L for his unit of lift as his model had a span of 1 m. Thus in Fig. 9, $C_L = C_l$.

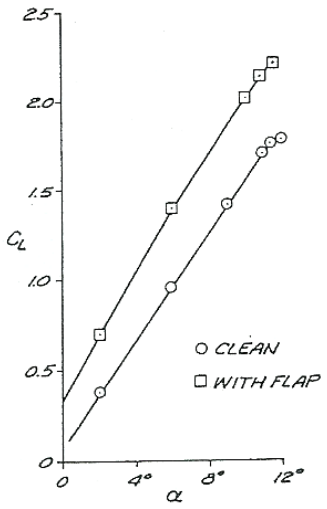

(a) Liebeck's findings (0.0125c flap)[6].

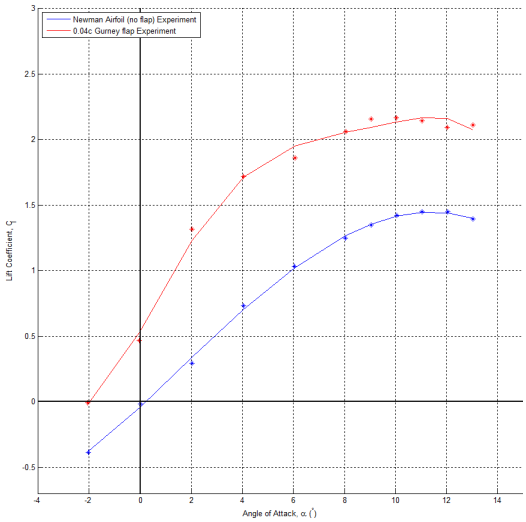

(b) Author's findings ($Re = 1.54 \times 10^5$).

Figure 9. Comparison of Results.

It can be seen from Fig. 9 that the clean (without flap) results are very similar and the slight difference lies in the variation due to the error within the experiment discussed above. Liebeck is very vague in his explanations of the exact method used for his experiment and his $0.0125c$ Gurney flap results are questionable. He obtained such a large $C_{l_{max}}$ for the $0.0125c$ Gurney flap that was only achieved in this research using a $0.04c$ Gurney flap. Previous research by Rayner[11] shows that as Gurney flap height is increased from 1.2% chord to 4% chord, there is a further increase in $C_{l_{max}}$. It seems optimistic that a $C_{l_{max}}$ of approximately 2.2 could be achieved with a $0.0125c$ Gurney flap.

Liebeck's theory of the flow behaviour around a Gurney flap was supported by the SOFV results. He stated that the addition of a Gurney flap would delay separation by creating an increase in the suction force on the upper side of the airfoil caused by the effective camber of the Gurney flap. This was found to be true.

Liebeck's statement that 'Gurney flaps of length greater than 1.25% chord will show a drag penalty'[6] was also supported by this research. The drag penalty in this research was found to be greater for the $0.04c$ Gurney flap than the $0.024c$ chord Gurney flap with increasing α. This again supports that there is a small range of angles of attack for which Gurney flaps are most efficient.

IV.D.3. Hypothesised Flow Structure

The flow structure around the $0.04c$ Gurney flap was examined using the results obtained from the CFD analysis. The results confirmed Liebeck's hypothesised flow structure around the Gurney flap. That of the two counter-rotating vortices that form just aft of the Gurney flap can be seen in Fig. 10. Fig. 10 shows the steady result at $\alpha = 0°$ and was selected as it is the CFD result that is the closest to the experimental result thus the phenomenon occurring in Fig. 9 is likely to be occurring in the experiment.

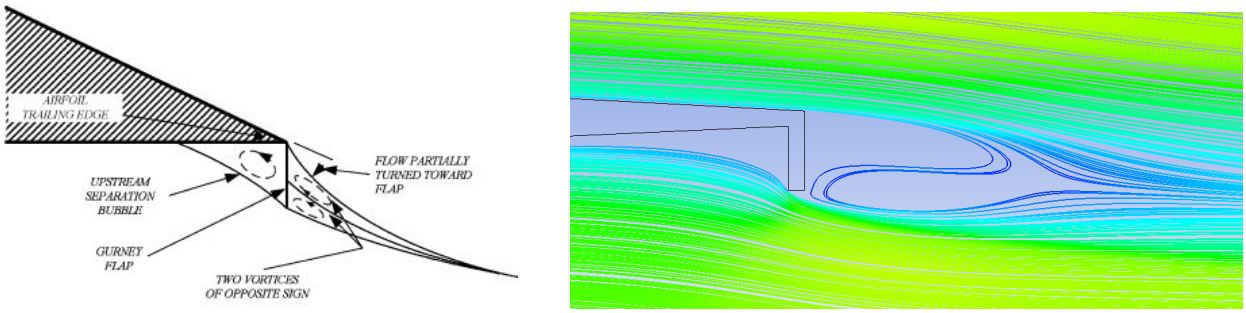

(a) Liebeck's hypothesised flow structure.

(b) CFD flow structure ($\alpha = 0°$).

Figure 10. Flow structure around a Gurney flap.

Since the steady result in Fig. 10 converged to the convergence criterion set (which were refined to obtain reliable convergence), it can be concluded that the flow structure at **zero degree angle of attack** is quasi-steady. This means that no large vortex shedding or Von Kármán vortex steet is forming aft of the Gurney flap thus validating Liebeck's hypothesised flow structure.

V. Conclusions

The Gurney flap improved the L/D ratio of the Newman airfoil significantly and extended the lift coefficient considerably due to the effective camber provided by the Gurney flap. The lift increase was found to be greater than the drag increase. However, the addition of a Gurney flap was found to only be effective for a small range of angles of attack and decreased the stall angle of the airfoil as the Gurney flap behaves like a deflected trailing edge flap. The Gurney flap alleviated stall for this airfoil compared to the no flap case as the lift coefficient post stall decreased more gradually than the no flap case. The surface-oil-flow-visualisation proved that the effective camber provided by the Gurney flap created a greater suction force on the upper side of the airfoil and explains the more gradual decrease in lift post stall. CFD simulations were conducted and compared to the experimental data thus validating the CFD. Previous research including the hypothesised trailing edge flow structure around a Gurney flap were also validated.

VI. Recommendations

From the findings of this research, recommendations into future research on Gurney flap aerodynamics are summarised herein. The Reynolds number should be increased to conduct a detailed comparison of full-scale aircraft. Various improvements to the CFD simulations should be made to improve the similarity of CFD and experimental results. For example, a thorough transient investigation of the unsteadiness of the wake flow at high angles of attack should be examined. Does this unsteadiness come from the wake flow or the flow separating forward of the Gurney flap? Through increasing the Gurney flap height, the optimum height *for this airfoil* can be found. The Newman airfoil shape should be modified so that the flow is 'turning' less around the leading edge thus reducing the adverse pressure gradient aft of the maximum t/c position to examine the effects on stall - Can an increase in stall angle be achieved by this simple modification?

Acknowledgements

First of all, I am grateful to my supervisors, A/Prof. Sudhir Gai and A/Prof. John Young, for their guidance and support throughout the duration of this research. I am incredibly thankful for the time they took from their work to lend a hand in mine. Their knowledge and passion for their research definitely brushed off on me! I would like to acknowledge the schools technical staff who have generously assisted in the experimental part of my research. And finally, the numerous friends and family who I couldn't have done this without. There are too many to list here although they know who they are.

References

[1]Gai S.L. & Palfrey R., *Influence of Trailing-Edge Flow Control on Airfoil Performance*, Journal of Aircraft, Vol. 40, No. 2, March-April 2003.

[2]Newman B., *Some Contributions to the Study of the Turbulent Boundary-Layer Near Separation*, Department of Supply, Aeronautical Research Consultative Committee, Sydney, Australia, 1951.

[3]Abbot I. & von Doenhoff A., *Theory of Wing Sections*, McGraw Hill, New York, 1949, pp 189.

[4]Jang C., Ross J. & Cummings R., *Computational Evaluation of an Airfoil with a Gurney Flap*, AIAA Paper 92-2708, June 1992.

[5]Jang C., Ross J. & Cummings R., *Numerical Investigation of an Airfoil with a Gurney Flap*, California Polytechnic State University and NASA Ames Research Centre, USA (unpublished).

[6]Liebeck R., *Design of Subsonic Airfoils for High Lift*, AIAA Paper 76-406, July 1978.

[7]Anderson J., *Fundamentals of Aerodynamics*, 5th ed., McGraw Hill, New York, 2011.

[8]Tickoo S., *CATIA V5R19 for Designers*, CADCIM Technologies, Indiana, USA, 2009.

[9]Barwick V., *Preparation of Calibration Curves, A Guide to Best Practice*, LGC Limited, London, UK, 2003, pp 4-22.

[10]Palfrey R., *Investigation of Trailing Edge Flow Control*, UNSW@ADFA, 2001 (unpublished).

[11]Rayner S., *Further Investigation of the Gurney flap*, UNSW@ADFA, 2002 (unpublished).

[12]Pope A. & Harper J., *Low-Speed Wind Tunnel Testing*, 1st ed., John Wiley & Sons, Inc., New York, 1966.

[13]Pope A. & Harper J., *Low-Speed Wind Tunnel Testing*, 2nd ed., John Wiley & Sons, Inc., New York, 1984.

[14]Rai W., Barlow J. & Pope A., *Low-Speed Wind Tunnel Testing*, 3rd ed., John Wiley & Sons, Inc., New York, 1999.

[15]Tu J., Yeoh G. & Liu C., *Computational Fluid Dynamics A Practical Approach*, 1st ed., Elsevier Inc., Burlington, USA, 2008.

[16]Versteeg H. & Malalasekera W., *An Introduction to Computational Fluid Dynamics The Finite Volume Method*, 2nd ed., Pearson Education Limited, England, 2007.

[17]Simmons J., *The Relationship Between the Base Pressure on a Bluff Body and the Velocity at Separation*, Aeronautical Journal, Vol. 78, July 1974, pp. 330-331.

[18]Roshko A., *On the Wake and Drag of Bluff Bodies*, Journal of Aeronautical Sciences, Vol. 22, No. 2, 1955, pp. 124-132.

[19]Myose R., Papadakis M. & Heron I., *Gurney Flap Experiments on Airfoils, Wings, and Reflection Plane Models*, Journal of Aircraft, Vol. 35, No. 2, 1998, pp. 206-211.